

Conversion of entangled states with nitrogen-vacancy centers coupled to microtoroidal resonators

Y. Q. JI,^{1,2} X. Q. SHAO,^{1,2} AND X. X. YI^{1,2,*}

¹Center for Quantum Sciences and School of Physics, Northeast Normal University, Changchun 130024, China

²Center for Advanced Optoelectronic Functional Materials Research, and Key Laboratory for UV Light-Emitting Materials and Technology of Ministry of Education, Northeast Normal University, Changchun 130024, China

*yixx@nenu.edu.cn

Abstract: We propose efficient schemes for converting three-photon, four-photon and five-photon GHZ state to a W state or Dicke state, respectively with the nitrogen-vacancy (N-V) centers via single-photon input-output process and cross-Kerr nonlinearities. The total success probability can be improved by iterating the conversion process for the case of three-photon and five-photon while it does not require iteration for converting four-photon GHZ state to a W state. The analysis of feasibility shows that our scheme is feasible for current experimental technology.

© 2021 Optical Society of America

OCIS codes: (270.0270) Quantum optics; (270.5585) Quantum information and processing; (190.3270) Kerr effect.

References and links

1. C. H. Bennett, G. Brassard, C. Crepeau, R. Jozsa, A. Peres, and W. K. Wootters, "Teleporting an unknown quantum state via dual classical and Einstein-Podolsky-Rosen channels," *Phys. Rev. Lett.* **70**, 1895-1899 (1993).
2. A. Karlsson and M. Bourennane, "Quantum teleportation using three-particle entanglement," *Phys. Rev. A* **58**, 4394-4400 (1998).
3. F. G. Deng, C. Y. Li, Y. S. Li, H. Y. Zhou, and Y. Wang, "Multiparty quantum-state sharing of an arbitrary two-particle state with Einstein-Podolsky-Rosen pairs," *Phys. Rev. A* **72**, 022338 (2005).
4. A. K. Ekert, "Quantum cryptography based on Bells theorem," *Phys. Rev. Lett.* **67**, 661-667 (1991).
5. C. H. Bennett, G. Brassard, and N. D. Mermin, "Quantum cryptography using any two nonorthogonal states," *Phys. Rev. Lett.* **68**, 557-559 (1992).
6. X. H. Li, F. G. Deng, and H. Y. Zhou, "Efficient quantum key distribution over a collective noise channel," *Phys. Rev. A* **78**, 022321 (2008).
7. M. Hillery, V. Bužek, and A. Berthiaume, "Quantum secret sharing," *Phys. Rev. A* **59**, 1829-1834 (1999).
8. L. Xiao, G. L. Long, F. G. Deng, and J. W. Pan, "Efficient multiparty quantum-secret-sharing schemes," *Phys. Rev. A* **69**, 052307 (2004).
9. F. L. Yan and T. Gao, "Quantum secret sharing between multiparty and multiparty without entanglement," *Phys. Rev. A* **72**, 012304 (2005).
10. B. Gu, L. L. Mu, L. G. Ding, C. Y. Zhang, and C. Q. Li, "Fault tolerant three-party quantum secret sharing against collective noise," *Opt. Commun.* **283**, 3099-3103 (2010).
11. G. L. Long and X. S. Liu, "Theoretically efficient high-capacity quantum-key-distribution scheme," *Phys. Rev. A* **65**, 032302 (2002).
12. X. H. Li, F. G. Deng, and H. Y. Zhou, "Improving the security of secure direct communication based on the secret transmitting order of particles," *Phys. Rev. A* **74**, 054302 (2006).
13. C. Wang, F. G. Deng, Y. S. Li, X. S. Liu, and G. L. Long, "Quantum secure direct communication with high-dimension quantum superdense coding," *Phys. Rev. A* **71**, 044305 (2005).
14. Z. X. Man, Z. J. Zhang, and Y. Li, "Deterministic secure direct communication by using swapping quantum entanglement and local unitary operations," *Chin. Phys. Lett.* **22**, 18-21 (2005).
15. A. D. Zhu, Y. Xia, Q. B. Fan, and S. Zhang, "Secure direct communication based on secret transmitting order of particles," *Phys. Rev. A* **73**, 022338 (2006).
16. W. Zhang, D. S. Ding, Y. B. Sheng, L. Zhou, B. S. Shi, G. C. Guo, "Quantum Secure Direct Communication with Quantum Memory," arXiv:1609.09184 (2016).
17. J. Y. Hu, B. Yu, M. Y. Jing, L. T. Xiao, S. T. Jia, G. Q. Qin, and G. L. Long, "Experimental quantum secure direct communication with single photons," *Science & Applications* **5**, e16144 (2016).
18. J. Pearson, G. R. Feng, C. Zheng, and G. L. Long, "Experimental quantum simulation of Avian Compass in a nuclear magnetic resonance system," *Science China Physics, Mechanics & Astronomy* **59**, 120312 (2016).

19. T. C. Li and Z. Q. Yin, "Quantum superposition, entanglement, and state teleportation of a microorganism on an electromechanical Oscillator," *Science Bulletin* **61**, 163-171 (2016).
20. W. H. Xu, X. Zhao, and G. L. Long, "Efficient generation of multi-photon W states by joint-measurement," *Nat. Science* **18**, 119-122 (2008).
21. X. Q. Shao, H. F. Wang, L. Chen, S. Zhang, Y. F. Zhao, and K. H. Yeon, "Converting two-atom singlet state into three-atom singlet state via quantum Zeno dynamics," *New. J. Phys.* **12**, 023040 (2010).
22. T. J. Wang, Y. Lu, and G. L. Long, "Generation and complete analysis of the hyperentangled Bell state for photons assisted by quantumdot spins in optical microcavities," *Phys. Rev. A* **86**, 042337 (2012).
23. X. Q. Shao, J. H. Wu, and X. X. Yi, "Dissipative stabilization of quantum-feedback-based multipartite entanglement with Rydberg atoms," *Phys. Rev. A* **95**, 022317 (2017).
24. R. Heilmanna, M. Gräfe, S. Nolte, and A. Szameita, "A novel integrated quantum circuit for high-order W-state generation and its highly precise characterization," *Science Bulletin* **60**, 96-100, (2015).
25. X. Q. Shao, L. Chen, S. Zhang, Y. F. Zhao, and K. H. Yeon, "Deterministic generation of arbitrary multi-atom symmetric Dicke states by a combination of quantum Zeno dynamics and adiabatic passage," *Europhys. Lett.* **90**, 50003 (2010).
26. Y. B. Sheng, J. Pan, R. Guo, L. Zhou, and L. Wang, "Efficient N-particle W state concentration with different parity check gates," *Science China Physics, Mechanics & Astronomy* **58**, 1-11 (2015).
27. X. Q. Shao, Z. H. Wang, H. D. Liu, and X. X. Yi, "Dissipative preparation of a tripartite singlet state in coupled arrays of cavities via quantum feedback control," *Phys. Rev. A* **94**, 032307 (2016).
28. Z. Wang, C. Zhang, Y. F. Huang, B. H. Liu, C. F. Li, and G. C. Guo, "Experimental verification of genuine multipartite entanglement without shared reference frames," *Science Bulletin* **61**, 714-719 (2016).
29. W. Dür, G. Vidal, and J. I. Cirac, "Three qubits can be entangled in two inequivalent ways," *Phys. Rev. A* **62**, 062314 (2000).
30. A. Acín, D. Bruß, M. Lewenstein, and A. Sanpera, "Classification of mixed three-qubit states," *Phys. Rev. Lett.* **87**, 040401 (2001).
31. N. Gisin and S. Massar, "Optimal Quantum Cloning Machines," *Phys. Rev. Lett.* **79**, 2153 (1997).
32. M. Murao, D. Jonathan, M. B. Plenio, and V. Vedral, "Quantum telecloning and multiparticle entanglement," *Phys. Rev. A* **59**, 156 (1999).
33. A. S. Zheng, J. H. Li, R. Yu, X. Y. Lǎij, and Y. Wu, "Generation of Greenberger-Horne-Zeilinger state of distant diamond nitrogen-vacancy centers via nanocavity input-output process," *Opt. Express* **20**, 16902-16912 (2012).
34. B. C. Ren and G. L. Long, "General hyperentanglement concentration for photon systems assisted by quantumdot spins inside optical microcavities," *Opt. Express* **22**, 6547-6561 (2014).
35. N. K. Yu, C. Guo, and R. Y. Duan, "Obtaining aW state from a Greenberger-Horne-Zeilinger state via Stochastic local operations and classical communication with a rate approaching unity," *Phys. Rev. Lett.* **112**, 160401 (2014).
36. X. Y. Lü, P. J. Song, J. B. Liu, and X. X. Yang, "N-qubit W state of spatially separated single molecule magnets," *Opt. Express* **17**, 14298-14311 (2009).
37. J. Wang, Q. Zhang, and C. J. Tang, "Quantum Secure Communication Scheme with W State," *Commun. Theor. Phys.* **48**, 637 (2007).
38. W. Liu, Y. B. Wang, and Z. T. Jiang, "An efficient protocol for the quantum private comparison of equality with W state," *Opt. Commun.* **284**, 3160 (2011).
39. P. Walther, K. J. Resch, and A. Zeilinger, "Local conversion of Greenberger-Horne-Zeilinger states to approximate W states," *Phys. Rev. Lett.* **94**, 240501 (2005).
40. T. Tashima, T. Wakatsuki, S. K. özdemir, T. Yamamoto, M. Koashi, and N. Imoto, "Local transformation of two Einstein-Podolsky-Rosen photon pairs into a three-photon W state," *Phys. Rev. Lett.* **102**, 130502 (2009).
41. H. F. Wang, S. Zhang, A. D. Zhu, X. X. Yi, and K. H. Yeon, "Local conversion of four Einstein-Podolsky-Rosen photon pairs into four-photon polarization-entangled decoherence-free states with non-photon-number-resolving detectors," *Opt. Express* **19**, 25433-25440 (2011).
42. J. Song, X. D. Sun, Q. X. Mu, L. L. Zhang, Y. Xia, and H. S. Song, "Direct conversion of a four-atom W state to a Greenberger-Horne-Zeilinger state via a dissipative process," *Phys. Rev. A* **88**, 024305 (2013).
43. G. Y. Wang, D. Y. Wang, W. X. Cui, H. F. Wang, A. D. Zhu, and S. Zhang, "Direct conversion of a three-atom W state to a Greenberger-Horne-Zeilinger state in spatially separated cavities," *J. Phys. B: Atom. Molec. Opt. Phys.* **49**, 065501 (2016).
44. W. X. Cui, S. Hu, H. F. Wang, A. D. Zhu, and S. Zhang, "Deterministic conversion of a four-photon GHZ state to a W state via homodyne measurement," *Opt. Express* **24**, 15319-15327 (2016).
45. B. Dayan, A. S. Parkins, T. Aoki, E. P. Ostby, K. I. Vahala, and H. J. Kimble, "A photon turnstile dynamically regulated by one atom," *Science* **319**, 1062-1065 (2008).
46. Y. S. Park, A. K. Cook, and H. Wang, "Cavity QED with diamond nanocrystals and silica microspheres," *Nano Lett.* **6**, 2075-2079 (2006).
47. M. Larsson, K. N. Dinyari, and H. Wang, "Composite optical microcavity of diamond nanopillar and silica microsphere," *Nano Lett.* **9**, 1447-1450 (2009).
48. R. J. Barbour, K. N. Dinyari, and H. Wang, "A composite microcavity of diamond nanopillar and deformed silica microsphere with enhanced evanescent decay length," *Opt. Express* **18**, 18968-18974 (2010).
49. F. Jelezko, T. Gaebl, I. Popa, M. Domhan, A. Gruber, and J. Wrachtrup, "Observation of coherent oscillation of a

- single nuclear spin and realization of a two-qubit conditional quantum gate,” *Phys. Rev. Lett.* **93**, 130501 (2004).
50. T. Gaebel, M. Domhan, I. Popa, C. Wittmann, P. Neumann, F. Jelezko, J. R. Rabeau, N. Stavrias, A. D. Greentree, S. Praver, J. Meijer, J. Twamley, P. R. Hemmer, and J. Wrachtrup, “Room-temperature coherent coupling of single spins in diamond,” *Nat. Phys.* **2**, 408-413 (2006).
 51. C. Santori, P. E. Barclay, K. M. C. Fu, and R. G. Beausoleil, “Vertical distribution of nitrogen-vacancy centers in diamond formed by ion implantation and annealing,” *Phys. Rev. B* **79**, 125313 (2009).
 52. C. Santori, D. Fattal, S. M. Spillane, M. Fiorentino, R. G. Beausoleil, A. D. Greentree, P. Olivero, M. Draganski, J. R. Rabeau, P. Reichart, S. Rubanov, D. N. Jamieson, and S. Praver, “Coherent population trapping in diamond N-V centers at zero magnetic field,” *Opt. Express* **14**, 7986-7994 (2006).
 53. E. Togan, Y. Chu, A. S. Trifonov, L. Jiang, J. Maze, L. Childress, M. V. G. Dutt, A. S. Sørensen, P. R. Hemmer, A. S. Zibrov, and M. D. Lukin, “Quantum entanglement between an optical photon and a solid-state spin qubit,” *Nature* **466**, 730-734 (2010).
 54. Q. Chen, W. L. Yang, M. Feng, and J. F. Du, “Entangling separate nitrogen-vacancy centers in a scalable fashion via coupling to microtoroidal resonators,” *Phys. Rev. A* **83**, 054305 (2011).
 55. J. H. An, M. Feng, and C. H. Oh, “Quantum-information processing with a single photon by an input-output process with respect to low-Q cavities,” *Phys. Rev. A* **79**, 032303 (2009).
 56. C. Y. Hu, W. J. Munro, and J. G. Rarity, “Deterministic photon entangler using a charged quantum dot inside a microcavity,” *Phys. Rev. B* **78**, 125318 (2008).
 57. J. Song, Y. Xia, and H. S. Song, “Quantum gate operations using atomic qubits through cavity input-output process,” *Europhys. Lett.* **87**, 50005 (2009).
 58. K. Nemoto and W. J. Munro, “Nearly Deterministic Linear Optical Controlled-NOT Gate,” *Phys. Rev. Lett.* **93**, 250502 (2004).
 59. S. D. Barrett, P. Kok, K. Nemoto, R. G. Beausoleil, W. J. Munro, and T. P. Spiller, “Symmetry analyzer for nondestructive Bell-state detection using weak nonlinearities,” *Phys. Rev. A* **71**, 060302 (2005).
 60. W. J. Munro, K. Nemoto, R. G. Beausoleil, and T. P. Spiller, “High-efficiency quantum-nondemolition single-photon-number-resolving detector,” *Phys. Rev. A* **71**, 033819 (2005).
 61. P. E. Barclay, K. M. C. Fu, C. Santori, and R. G. Beausoleil, “Chip-based microcavities coupled to nitrogenvacancy centers in single crystal diamond,” *Appl. Phys. Lett.* **95**, 191115 (2009).
 62. S. D. Barrett, P. Kok, K. Nemoto, R. G. Beausoleil, W. J. Munro, and T. P. Spiller, “Symmetry analyzer for nondestructive Bell-state detection using weak nonlinearities,” *Phys. Rev. A* **71**, 060302 (2005).
 63. P. R. Hemmer, A. V. Turukhin, M. S. Shahriar, and J. A. Musser, “Raman-excited spin coherences in nitrogen-vacancy color centers in diamond,” *Opt. Lett.* **26**, 361 (2001).
 64. M. S. Shahriar, P. R. Hemmer, S. Lloyd, P. S. Bhatia, and A. E. Craig, “Solid-state quantum computing using spectral holes,” *Phys. Rev. A* **66**, 032301 (2002).
-

1. Introduction

It is well known that quantum entanglement is the basic resource in quantum information processing (QIP). It is widely used in quantum teleportation [1–3], quantum key distribution [4–6], quantum secret sharing [7–10] and quantum secure direct communication [11–17]. Furthermore, it is even considered as an important effect in living biological bodies in recent years, for instance, the entanglement may be related to Avian compass [18], and the entanglement and teleportation using living cell is also possible [19]. Owing to its importance, many theoretical and experimental efforts for generating entanglement have been one focus of the current study [20–28]. There are two most common classes of entangled states for a multipartite system, i.e., GHZ state and W state, which cannot be converted to each other by local operations and classical communication (LOCC) [29, 30]. For the GHZ state, the entanglement completely degrades with the loss of any one of the qubits. However, the W state is robust against the loss of one qubit, when one qubit is discarded, the remaining qubits can be still entangled with each other. Due to this two kinds of entangled states can be used for performing different tasks in QIP [31–38], naturally, the question arises: how the two kinds of entanglement can be converted into each other?

Recently, many research have been focused on the conversion between GHZ state and W state [39–44]. Walther *et al.* described a specific method based on local positive operator valued measures and classical communication to convert a N -qubit GHZ state into an approximate W state experimentally and implemented this scheme in the 3-qubit case in 2005 [39]. Subsequently, Tashima *et al.* proposed and experimentally demonstrated a transformation of two EPR photon pairs distributed among three parties into a three-photon W state using LOCC in 2009 [40]. More

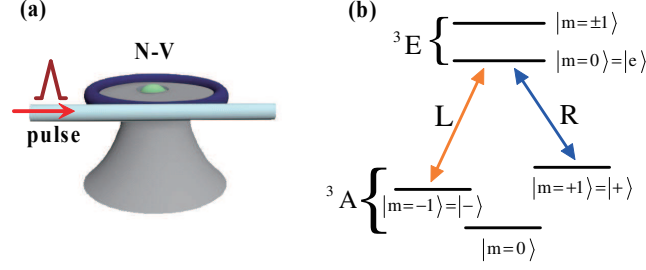


Fig. 1. Diagrammatic illustration of basic model. (a) An N-V center is confined to a MTR and a single photon pulse is introduced to interact with the N-V center. (b) The electron energy level configuration of the N-V center and relevant transition coupling with corresponding polarization photon.

recently, Wang *et al.* proposed a linear-optics-based scheme for local conversion of four EPR photon pairs distributed among five parties into four-photon polarization-entangled decoherence-free states [41]. Song *et al.* proposed a scheme for converting a W state into a GHZ state with a deterministic probability through a dissipative dynamics process [42]. These works provides a new way to implement the conversion of entangled states.

As a promising candidate for the quantum computer, nitrogen-vacancy (N-V) centers in diamond are coupled to the microresonator with a quantized whispering-gallery mode (WGM) [45–48] shows great advantage and practical feasibility as they have a long lifetime even at room temperature and can be manipulated and detected by optical field or microwave [49, 50]. Hence, the N-V center, consists of nearest-neighbor pair of a nitrogen atom substituted for a carbon atom and a lattice vacancy in diamond, becomes one of the most potential carrier of quantum information due to these characteristics.

Motivated by the former works, we suggest a high-fidelity CNOT gate between two photons can be constructed resorting to N-V center through microtoroidal resonator (MTR) assisted single-photon input-output process. A high fidelity can be achieved. And the schemes of entangled states conversion are presented for converting three-photon, four-photon and five-photon GHZ state to a W state or Dicke state by applying the CNOT gate and cross-Kerr nonlinearities. The schemes has the following advantages: the minimum success probability of conversion a three-photon GHZ state to a W state is $3/4$, while by iterating the conversion process, the total success probability can be to unit, but the conversion for four-photon GHZ to a W state does not need iteration. For five-photon GHZ state, the total success probability for converting to a W state can be to $1/3$ by iterating the conversion process. Meanwhile, we can obtain a Dicke state $|D_5^{(2)}\rangle$ with the success probability $2/3$.

2. Physical model

At the beginning, we provide a brief background on the basic unit of the N-V centers and microcavity system. In order to facilitate manipulating and extending the MTR-N-V center system, the N-V center should be close to the surface of diamond and the fibre transmitting input pulse is close to the resonator [51]. As illustrated in Figs. 1(a), an N-V center is fixed on the surface of a MTR and can be coupled to the cavity mode. And the electron energy level configuration of N-V center is shown in Figs. 1(b). The zero-field splitting and the Zeeman splitting from an external magnetic field determine the ground levels $|{}^3A, m_s = 0\rangle$, $|-\rangle$ and $|+\rangle$ [52, 53]. The information is encoded on the ground states $|-\rangle$ and $|+\rangle$. The excited state $|A_2\rangle$ acts as auxiliary level $|e\rangle$ [53, 54]. The level transition between $|-\rangle$ ($|+\rangle$) and $|e\rangle$ is resonantly coupled to the left (right) circularly polarized photon $|L\rangle$ ($|R\rangle$) in MTR.

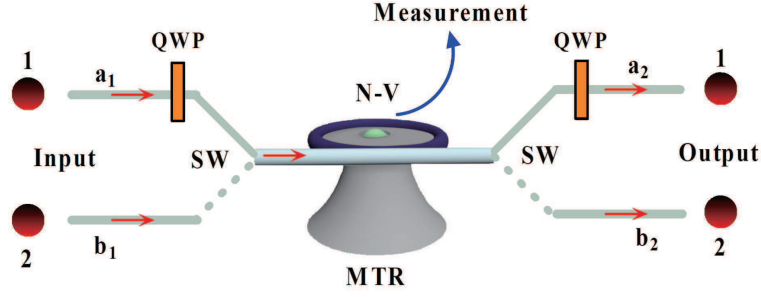


Fig. 2. Schematic of deterministic photonic CNOT gate with an N-V center confined to a MTR. QWP is a quarter-wave plate which performs the transformations $|R\rangle \rightarrow \frac{1}{\sqrt{2}}(|R\rangle + |L\rangle)$, $|L\rangle \rightarrow \frac{1}{\sqrt{2}}(|R\rangle - |L\rangle)$, and SW is optical switch.

Consider a single-photon pulse with frequency ω_p input in a MTR cavity with the mode frequency ω_c . Under the assumption of weak excitation limit, i.e., $\langle \sigma_z \rangle = 1$. So, the Langevin equations of motion are solvable for the lowering operators of the cavity and the N-V center. According to the cavity input-output process [55–57] and adiabatical elimination of the cavity mode leads to the reflection coefficient as [55]

$$r(\omega_p) = \frac{[i(\omega_c - \omega_p) - \frac{\kappa}{2}] [i(\omega_0 - \omega_p) + \frac{\gamma}{2}] + g^2}{[i(\omega_c - \omega_p) + \frac{\kappa}{2}] [i(\omega_0 - \omega_p) + \frac{\gamma}{2}] + g^2} \quad (1)$$

where ω_0 is the transition frequency between energy levels $|-\rangle$ and $|e\rangle$. κ and γ are the cavity damping rate and the N-V center dipolar decay rate, respectively, and g is the coupling strength of the cavity to the N-V center. If the N-V centers are uncoupled from the cavity, i.e. $g = 0$, Eq. (1) changes to

$$r_0(\omega_p) = \frac{i(\omega_c - \omega_p) - \frac{\kappa}{2}}{i(\omega_c - \omega_p) + \frac{\kappa}{2}} \quad (2)$$

If a single polarized photon $|L\rangle$ is reflected from a MTR cavity after running into an N-V center prepared in $|-\rangle$ or $|+\rangle$, it will experience a phase shift $e^{i\phi}$ or $e^{i\phi_0}$ from Eq. (1) or (2) owing to optical Faraday rotation, respectively. While if a single $|R\rangle$ polarized photon is reflected, it will experience a phase shift $e^{i\phi_0}$ regardless of what the electronic spin states are. Choosing the resonant condition $\omega_c = \omega_0 = \omega_p$ and $g^2 \geq 25\kappa\gamma$, then

$$r(\omega_p) \simeq 1, \quad r_0(\omega_p) = -1. \quad (3)$$

In conclusion, after a π phase shifter on the photon output path, the systemic state between the photon and the N-V centers can be expressed as

$$\begin{aligned} |R\rangle|+\rangle &\rightarrow |R\rangle|+\rangle, & |R\rangle|-\rangle &\rightarrow |R\rangle|-\rangle, \\ |L\rangle|+\rangle &\rightarrow |R\rangle|+\rangle, & |L\rangle|-\rangle &\rightarrow -|L\rangle|-\rangle. \end{aligned} \quad (4)$$

In the following, we investigate how to construct a deterministic CNOT gate and implement conversion of entangled states between photonic qubits.

3. Implementing of deterministic CNOT gate for photonic qubits

Consider two photons initially prepared in an arbitrary state $\psi_p = \alpha|RR\rangle + \beta|RL\rangle + \gamma|LR\rangle + \delta|LL\rangle$, where $|\alpha|^2 + |\beta|^2 + |\delta|^2 + |\gamma|^2 = 1$, and N-V center in the state $\psi_N = \frac{1}{\sqrt{2}}(|+\rangle + |-\rangle)$. Photon 2

acts as control qubit and photon 1 acts as target qubit. The schematic is shown in Fig. 2. The two photons 1 and 2 come in succession to the MTR. The action of the quarter-wave plate (QWP) is given by transformation $|R\rangle \rightarrow \frac{1}{\sqrt{2}}(|R\rangle + |L\rangle)$ and $|L\rangle \rightarrow \frac{1}{\sqrt{2}}(|R\rangle - |L\rangle)$. The optical switch (SW) controls the photon 1 passing through the MTR firstly and then the photon 2. c-PBS is circular polarization beam splitter which transmits the right-circular polarization photon $|R\rangle$ and reflects the left-circular polarization photon $|L\rangle$. In Fig. 2, before the photon 2 enters into the MTR, a Hadamard gate operation, which can be achieved by a $\pi/2$ microwave pulse, is performed on N-V center to accomplish the transformation $|+\rangle \rightarrow \frac{1}{\sqrt{2}}(|+\rangle + |-\rangle)$ and $|-\rangle \rightarrow \frac{1}{\sqrt{2}}(|+\rangle - |-\rangle)$. After the photon 2 passing through the MTR, the N-V center is rotated by the Hadamard gate transformation again. Finally, the total state of two photons with one N-V center is transformed into

$$\begin{aligned} \psi_p \otimes \psi_N \rightarrow & \frac{1}{\sqrt{2}}(\alpha|RR\rangle + \beta|LL\rangle + \gamma|LR\rangle + \delta|RL\rangle)_{1,2} \otimes |+\rangle \\ & + \frac{1}{\sqrt{2}}(\alpha|LR\rangle + \beta|RL\rangle + \gamma|RR\rangle + \delta|LL\rangle)_{1,2} \otimes |-\rangle. \end{aligned} \quad (5)$$

After the measurement performed on the N-V center, the CNOT gate between photons 1 and 2, which is unequivocally associated to the measurement results of the N-V center in the $|+\rangle$, $|-\rangle$ basis, is achieved (see Table 1).

Table 1. The measurement results and corresponding single-qubit operations on photons 1 and 2 in the case of the CNOT gate.

N-V center	Photons 1 and 2	Operations
$ +\rangle$	$\alpha RR\rangle + \beta LL\rangle + \gamma LR\rangle + \delta RL\rangle$	$I^1 \otimes I^2$
$ -\rangle$	$\alpha LR\rangle + \beta RL\rangle + \gamma RR\rangle + \delta LL\rangle$	$\sigma_x^1 \otimes I^2$

4. Conversion of entangled states

In this section, we illustrate how to convert a GHZ state to a W state in a deterministic way based on single-photon input-output process and cross-Kerr nonlinearity.

4.1. Conversion of a three-photon GHZ state to a three-photon W state

Assume that photons 1, 2 and 3, as shown in Fig. 3, are in the following state

$$|\psi\rangle_0 = \frac{1}{\sqrt{2}}(|RLR\rangle + |LRL\rangle)|\alpha\rangle, \quad (6)$$

then the photons firstly pass through a CNOT gate, where photon 2 act as the control qubit and photon 3 act as the target qubit. Then the photon 3 passes through a HWP, whose action is to make $|R\rangle \rightarrow |L\rangle$ and $|L\rangle \rightarrow |R\rangle$, and a QWP, performing the transformations $|R\rangle \rightarrow \frac{1}{\sqrt{2}}(|R\rangle + |L\rangle)$ and $|L\rangle \rightarrow \frac{1}{\sqrt{2}}(|R\rangle - |L\rangle)$ in sequence. At last, the photons pass through a CNOT gate, with photon 3 being control qubit and photon 1 being target qubit. The resulting state of the whole system is given by

$$|\psi\rangle_1 = \frac{1}{2}(|RLR\rangle + |LRR\rangle + |RRL\rangle + |LLL\rangle)|\alpha\rangle. \quad (7)$$

After the three-photon state and a coherent probe beam couple with a cross-Kerr nonlinearity medium, the evolution of the whole system can be described as

$$|\psi\rangle_2 = \frac{1}{2}(|RLR\rangle + |LRR\rangle + |RRL\rangle)|\alpha e^{i\theta}\rangle + \frac{1}{2}|LLL\rangle|\alpha e^{i3\theta}\rangle, \quad (8)$$

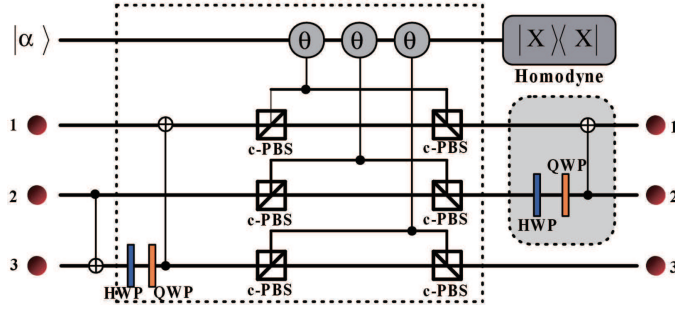


Fig. 3. Schematic setup for converting a three-photon GHZ state to a three-photon W state. Here HWP denotes a half-wave plate which performs the transformations $|R\rangle \rightarrow |L\rangle$ and $|L\rangle \rightarrow |R\rangle$. QWP denotes a quarter-wave plate which performs the transformations $|R\rangle \rightarrow \frac{1}{\sqrt{2}}(|R\rangle + |L\rangle)$ and $|L\rangle \rightarrow \frac{1}{\sqrt{2}}(|R\rangle - |L\rangle)$. c-PBS denotes a polarization beam splitter in the circular basis that transmits R photons and reflects L photons. The action of the cross-Kerr nonlinearity puts a phase shift θ on the probe beam only if a photon was present in that mode.

For cross-Kerr nonlinearity, the Hamiltonian can be described as $H = \hbar\chi a_s^\dagger a_s a_p^\dagger a_p$ [58–60], here a_s^\dagger and a_p^\dagger are the creation operations, a_s and a_p are the destruction operations. χ is the coupling strength of the nonlinearity. For a signal state $|\phi\rangle_s = \alpha|0\rangle_s + \beta|1\rangle_s$ ($|0\rangle_s$ and $|1\rangle_s$ denote that there are no photon and one photon, respectively) and a coherent probe beam in the state $|\alpha\rangle$ couple with a cross-Kerr nonlinearity medium, the systemic evolve as $\alpha|0\rangle_s|\alpha\rangle + \beta|1\rangle_s|\alpha e^{i\theta}\rangle$, where $\theta = \chi t$ and t is interaction time. The coherent probe beam picks up a phase shift directly proportional to the number of photons. Hence, for the Eq. (8), one can find immediately that $|RLR\rangle$, $|LRR\rangle$ and $|RRL\rangle$ cause the coherent beam $|\alpha\rangle$ to pick up a phase shift θ , and $|LLL\rangle$ to pick up a phase shift 3θ . The different phase shifts can be distinguished by a general X homodyne measurement. If we obtains the state $|\alpha e^{i\theta}\rangle$, the three photons are in the maximally entangled state, with the probability of $3/4$. If we obtains the state $|\alpha e^{i3\theta}\rangle$, the three photons are in the state $|LLL\rangle$.

For the state $|LLL\rangle$, we let the second photon pass through a HWP, QWP and perform a CNOT gate on photons 1 and 2, with photon 2 act as control qubit and photon 1 act as target qubit. Then the state $|LLL\rangle$ becomes $\frac{1}{\sqrt{2}}(|RLL\rangle + |LRL\rangle)$. After that, we perform the operations in dashed box in Fig. 3. We can recover Eq. (8) again. So it still can be used for conversion. At last, we convert the three photons to a W state. The success probability of obtaining W state for the second round is $P = \frac{1}{4} \times \frac{3}{4} = \frac{3}{16}$. That is, by iterating the conversion process n times, the total success probability of this conversion is

$$P = \sum_{m=1}^n \left(\frac{1}{4}\right)^{m-1} \times \frac{3}{4}, \quad (9)$$

It is obvious that the success probability increases with the increasing of the iteration time. When the iteration time equal to 4, the success probability can reach 99.6%.

4.2. Conversion of a four-photon GHZ state to a four-photon W state

For a four-photon GHZ state convert to a four-photon W state as shown Fig. 4. We assume the four photons are in the state

$$|\psi\rangle_0 = \frac{1}{\sqrt{2}}(|RLRR\rangle + |LRLR\rangle)|\alpha\rangle, \quad (10)$$

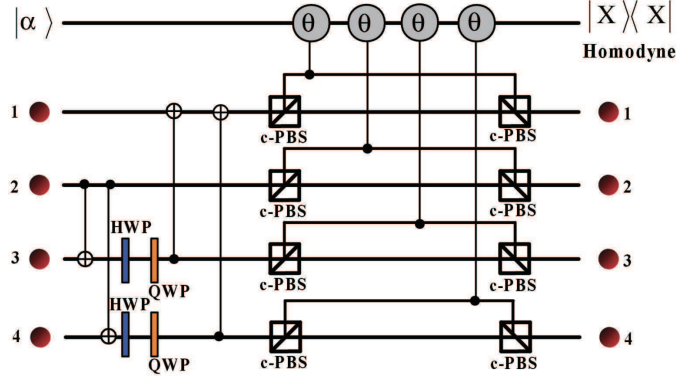


Fig. 4. Schematic setup for converting a four-photon GHZ state to a four-photon W state.

After the four photons pass through the first two CNOTs, the systemic state becomes

$$|\psi\rangle_1 = \frac{1}{\sqrt{2}}(|RLLL\rangle + |LRLL\rangle)|\alpha\rangle, \quad (11)$$

Then the photons pass through HWPs, QWPs and the second two CNOTs, the systemic state becomes

$$|\psi\rangle_3 = \frac{1}{2\sqrt{2}}(|RRRL\rangle + |RRLR\rangle + |RLRR\rangle + |LRRR\rangle + |RLLL\rangle + |LRLL\rangle + |LLRL\rangle + |LLLR\rangle)|\alpha\rangle, \quad (12)$$

After the single photon pulse and a coherent probe beam in the state $|\alpha\rangle$ couple with a cross-Kerr nonlinearity medium, the evolution of the whole system can be described as

$$\begin{aligned} |\psi\rangle_3 = & \frac{1}{2\sqrt{2}}(|RRRL\rangle + |RRLR\rangle + |RLRR\rangle + |LRRR\rangle)|\alpha e^{i\theta}\rangle \\ & + \frac{1}{2\sqrt{2}}(|RLLL\rangle + |LRLL\rangle + |LLRL\rangle + |LLLR\rangle)|\alpha e^{i3\theta}\rangle, \end{aligned} \quad (13)$$

From the Eq. (13), one can see that whatever the measurement result is $|\alpha e^{i\theta}\rangle$ or $|\alpha e^{i3\theta}\rangle$, the standard four-photon W state can be obtained. Hence, the success probability for conversion of a four-photon GHZ state to a four-photon W state can reach unit.

4.3. Conversion of a five-photon GHZ state to a five-photon W state and $|D_5^{(2)}\rangle$ state

For a five-photon GHZ state convert to a five-photon W state as shown Fig. 5. We assume the five photons are in the state

$$|\psi\rangle_0 = \frac{1}{\sqrt{2}}(|RLRRR\rangle + |LRLLL\rangle)|\alpha\rangle, \quad (14)$$

After the photons pass through the first three CNOTs, the systemic state becomes

$$|\psi\rangle_1 = \frac{1}{\sqrt{2}}(|RLLLL\rangle + |LRLLL\rangle)|\alpha\rangle, \quad (15)$$

Then the photons pass through HWPs, QWPs and the second three CNOTs, the systemic state becomes

$$|\psi\rangle_2 = \frac{1}{4}(|LRRRR\rangle + |RLRRR\rangle + |RRLRR\rangle + |RRRLR\rangle + |RRRRL\rangle + |LLLLL\rangle)$$

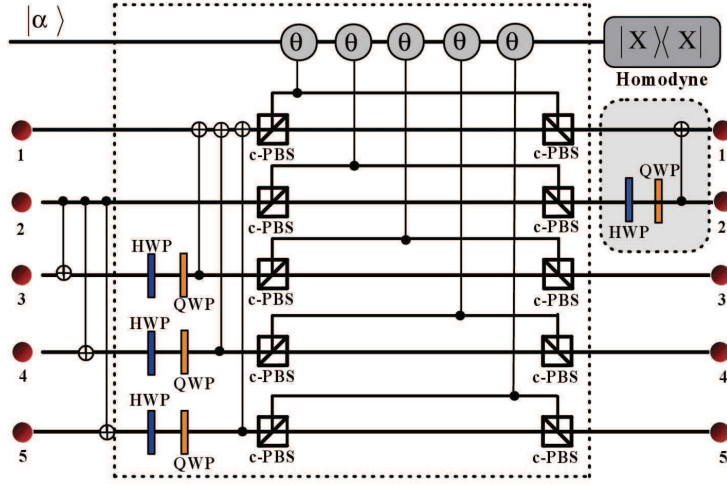


Fig. 5. Schematic setup for converting a five-photon GHZ state to a five-photon W state and $|D_5^{(2)}\rangle$ state.

$$\begin{aligned}
& +|LLRRL\rangle + |LLRLR\rangle + |RLRLL\rangle + |LLLRR\rangle + |RLLRL\rangle + |RLLLR\rangle \\
& +|LRRLL\rangle + |LRLRL\rangle + |LRLLR\rangle + |RRLLL\rangle)|\alpha\rangle
\end{aligned} \quad (16)$$

Then the photon pulse and a coherent probe beam couple with a cross-Kerr nonlinearity medium, the whole systemic state can be described as

$$\begin{aligned}
|\psi\rangle_3 = & \frac{1}{4}(|LRRRR\rangle + |RLRRR\rangle + |RRLRR\rangle + |RRRLR\rangle + |RRRRL\rangle)|\alpha e^{i\theta}\rangle + \frac{1}{4}|LLLLL\rangle|\alpha e^{i5\theta}\rangle \\
& + \frac{1}{4}(|LLRRL\rangle + |LLRLR\rangle + |RLRLL\rangle + |LLLRR\rangle + |RLLRL\rangle + |RLLLR\rangle \\
& + |LRRLL\rangle + |LRLRL\rangle + |LRLLR\rangle + |RRLLL\rangle)|\alpha e^{i3\theta}\rangle,
\end{aligned} \quad (17)$$

If the probe mode is in the state $|\alpha e^{i\theta}\rangle$, that is, the probe beam only picks up a phase shift θ , the signal mode will be projected to

$$|\varphi\rangle_1 = \frac{1}{\sqrt{5}}(|LRRRR\rangle + |RLRRR\rangle + |RRLRR\rangle + |RRRLR\rangle + |RRRRL\rangle). \quad (18)$$

The conversion of a five-photon GHZ state to a W state will succeed, which takes place with the probability $5/16$. However, if the probe mode is in the state $|\alpha e^{i3\theta}\rangle$, the signal mode will be projected to

$$\begin{aligned}
|\varphi\rangle_2 = & \frac{1}{\sqrt{10}}(|LLRRL\rangle + |LLRLR\rangle + |RLRLL\rangle + |LLLRR\rangle + |RLLRL\rangle + |RLLLR\rangle \\
& + |LRRLL\rangle + |LRLRL\rangle + |LRLLR\rangle + |RRLLL\rangle)
\end{aligned} \quad (19)$$

Then it converts to another kind of entangled state, i.e., Dicke state $|D_5^{(2)}\rangle$. The success probability of obtaining the $|D_5^{(2)}\rangle$ state is $5/8$. If the probe mode is in the state $|\alpha e^{i5\theta}\rangle$, the signal mode will be projected to $|LLLLL\rangle$. Here, we use the previous method, i.e., we let the second photon pass through a HWP, QWP and perform a CNOT gate on photons 1 and 2. Then the state $|LLLLL\rangle$ becomes $\frac{1}{\sqrt{2}}(|RLLLL\rangle + |LRLLL\rangle)$. After that, we perform the operations in dashed box in Fig. 5. We can obtain the Eq. (17) again. So it is still can be used for conversion. At last, after n

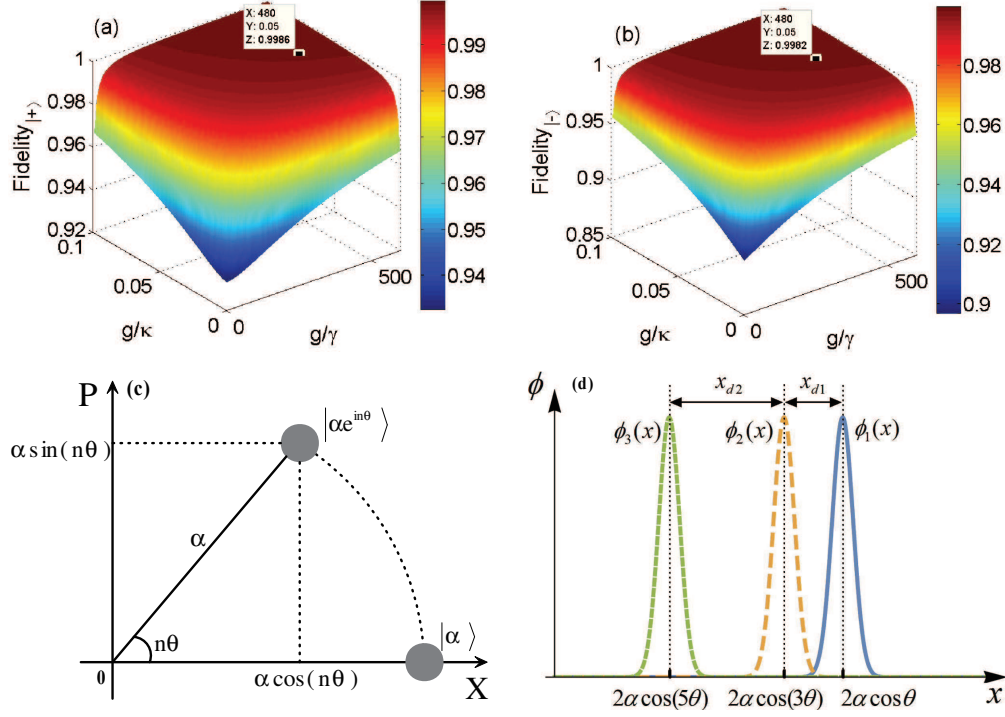


Fig. 6. (a) The fidelity of the CNOT gate versus the g/κ and g/γ corresponding to the measurement result of the N-V center is $|+\rangle$. (b) The fidelity of the CNOT gate versus the g/κ and g/γ corresponding to the N-V center is $|-\rangle$. (c) Schematic phase space illustration of the coherent state $|\alpha e^{in\theta}\rangle$. (d) Gaussian probability distribution for the result of the X quadrature homodyne measurement. The blue solid curve, yellow dashed curve and the green dashed curve correspond to $\phi(x, \alpha \cos \theta)$, $\phi(x, \alpha \cos 3\theta)$ and $\phi(x, \alpha \cos 5\theta)$, respectively. x_d is the distance between two peaks.

times iteration, the total success probability of obtaining W state is $P_W = \sum_{m=1}^n \left(\frac{1}{16}\right)^{m-1} \times \frac{5}{16}$ and the total success probability of obtaining $|D_5^{(2)}\rangle$ state is $P_D = \sum_{m=1}^n \left(\frac{1}{16}\right)^{m-1} \times \frac{10}{16}$. After many iterations, $P_W \approx \frac{1}{3}$ and $P_D \approx \frac{2}{3}$.

5. Analysis and discussion

The schemes for conversion of entangled states are all constructed with the CNOT gate and cross-Kerr nonlinearity. Therefore the fidelity of the CNOT gate and the error probability of the X homodyne measurement are crucial to the schemes of the conversion. Due to the imperfect coupling strength and leak rate will inevitably bring about slight influence on the reflectance of output photons. The interaction of the incident photon pulse and N-V center in Eq. (4) should be rewritten as

$$\begin{aligned} |R\rangle|+\rangle &\rightarrow -r_0(\omega_p)|R\rangle|+\rangle, & |R\rangle|-\rangle &\rightarrow -r_0(\omega_p)|R\rangle|-\rangle, \\ |L\rangle|+\rangle &\rightarrow -r_0(\omega_p)|R\rangle|+\rangle, & |L\rangle|-\rangle &\rightarrow r(\omega_p)|L\rangle|-\rangle. \end{aligned} \quad (20)$$

The fidelity is defined as $|\langle\psi_r|\psi_i\rangle|^2$ to check the performance of the CNOT gate, in which $|\psi_r\rangle$ and $|\psi_i\rangle$ represent the final state in the realistic condition and the ideal condition, respectively. The Figs. 6 (a) and 6(b) are the fidelities of the CNOT gate versus the g/κ and g/γ

corresponding to the measurement result of the N-V center is $|+\rangle$ and $|-\rangle$ respectively, and show our schemes can be achieved with high fidelities. In [61], the parameters are chosen as follows: $[g, \kappa, \gamma_{total}, \gamma_{ZPL}] = [0.3, 26, 0.013, 0.0004]$ GHz for a hybrid diamond-GaP microdisk system. Here, γ_{ZPL} is the zero phonon line (ZPL) emission spontaneous rate of an N-V center. By substituting these values, we have the fidelities for CNOT gate is 99.6% and 99.5% corresponding to the measurement result is $|+\rangle$ and $|-\rangle$ respectively. Therefore, it has an effect on the fidelities of the conversion. For example, in the process of conversion of a three-photon GHZ state to a three-photon W state, two CNOT gates need be performed, the fidelity can achieve 99.2%, even the iteration time equal to four, the fidelity can also achieve 95.7%. For conversion of a four-photon GHZ state to a four-photon W state, we need not the iteration, so four CNOT gates need be performed, the fidelity can achieve 98.4%. However, when the conversion of a five-photon GHZ state to a five-photon W state and Dicke state is iterated four times, the fidelity can only achieve 89.7%.

In addition, in order to completely distinguish $|\alpha e^{i\theta}\rangle$, $|\alpha e^{i3\theta}\rangle$ and $|\alpha e^{i5\theta}\rangle$, we adopt homodyne measurement on the coordinate space of the coherent state. The wave function of the coherent state $|\alpha e^{in\theta}\rangle$ in the coordinate space is $\phi(x, \alpha \cos(n\theta)) = (2\pi)^{-\frac{1}{4}} \exp[-\frac{1}{4}(x - 2\alpha \cos(n\theta))^2]$. Here, $\phi(x, \alpha \cos \theta) = \phi_1(x)$, $\phi(x, \alpha \cos 3\theta) = \phi_2(x)$ and $\phi(x, \alpha \cos 5\theta) = \phi_3(x)$, as shown in Figs. 6 (c) and 6 (d), are Gaussian probability amplitudes. Therefore, the three Gaussian curves with three peaks located at $2\alpha \cos \theta$, $2\alpha \cos 3\theta$ and $2\alpha \cos 5\theta$. The error probability can be obtained with the same method as in [62]. The small overlap between the two Gaussian curves amounts to the error probability, given by $P_{error} = \frac{1}{2} \text{erfc}\left(\frac{x_d}{2\sqrt{2}}\right)$, where x_d is the distance between two peaks with $x_{d1} = 2\alpha(\cos \theta - \cos 3\theta)$ and $x_{d2} = 2\alpha(\cos 3\theta - \cos 5\theta)$. As a very promising method for generating the form of nonlinearity required, we consider a two-dimensional photonic crystal waveguide constructed from diamond thin film with N-V centers fabricated in the center of the waveguide channel [63, 64] could provide a sufficiently large nonlinearity. For example, when the probe photon number $\alpha^2 = 1.3 \times 10^4$ and modest detunings, the cryogenic N-V-diamond system with 2×10^4 color centers can generate a phase shift of more than 0.1 rad per signal photon. Hence, the error probability for X homodyne measurement in our scheme is less than 10^{-5} , which makes the scheme is feasible in the experiment with weak cross-Kerr nonlinearities.

In conclusion, we have proposed a scheme, based on single-photon input-output process and cross-Kerr nonlinearities, that allowed to locally convert three-photon, four-photon and five-photon GHZ state to a W state or Dicke state via LOCC. The total success probability can be improved by iterating the conversion process for case of three-photon and five-photon. This method also can be used to convert a $(N>5)$ -photon GHZ state into W state or Dicke state. The proposed schemes have unique characteristics compared with the existing ones. The final analysis shows that our schemes are feasible and may have good performance in the current experimental conditions. We hope that our scheme could find some applications in the near future.

Acknowledgments

We would like to thank Dr. Zhao Jin for valuable discussions.

Funding

National Natural Science Foundation of China (NSFC) under Grants No. 11534002 and No. 61475033; Fundamental Research Funds for the Central Universities under Grants No. 2412016KJ004.